BNL-103719-2014-TECH
C-A/AP/502;BNL-103719-2013-IR

On the image in RHIC of AGS spin vector via the AtR

F. Meot

July 2013

Collider Accelerator Department
Brookhaven National Laboratory

U.S. Department of Energy
USDOE Office of Science (SC)

DISCLAIMER

BNL-103719-2013-IR

C-A/AP/502
July 2013

On the image in RHIC of AGS spin vector, via the AtR

F. Meot, H. Huang, N. Tsoupas

Collider-Accelerator Department
Brookhaven National Laboratory
Upton, NY 11973

On the image in RHIC of AGS $\vec{n}_0$, via the AtR

F. Méot, H. Huang, N. Tsoupas

BNL C-AD, Upton, LI, NY 11973

July 20th, 2013

Abstract

This note re-visits the transport of the spin $\vec{n}_0$ vector, from its periodic orientation in the AGS, to the downstream end of the Blue and Yellow RHIC ring injection kickers via the AGS extraction system and the AtR line. The goal is to verify the optimal injection energy into RHIC, in matter of spin matching.

This is done using newly computed OPERA 3-D field maps of the AGS cold snake, including a new setting of the cold snake solenoid as discussed in a companion Tech. Note (C-A/AP/485, July 2013), together with the machinery of the AGS and AtR models developed in the stepwise ray-tracing code Zgoubi.

Computing tools and methods employed in these investigations are discussed as well, in order to facilitate possible further checks or investigations.

Contents

1 Introduction

In preparation of RHIC Run 13, and in relation with a re-assessment of the AGS snake strengths as discussed in a companion Tech. Note, Ref. [1], the question was raised of the optimum extraction energy from the AGS with regard to the transport of the spin $\vec{n}_0$ vector, via the non-planar AtR line [1], Fig. 1, from its periodic, non-vertical, orientation at G10 extraction kicker in the AGS [2], to the downstream end of the Blue and Yellow RHIC ring injection kickers where it is expected to be as close as possible [3] to the periodic, vertical, RHIC $\vec{n}_0$. It was desired in particular to verify that the present extraction $G\gamma = 45.5$ does yield optimal matching of $\vec{n}_0$, considering that, due to the interleaved horizontal and vertical bends in the AtR, the image of the AGS $\vec{n}_0$ at RHIC injection point varies with both energy and AGS snake settings.

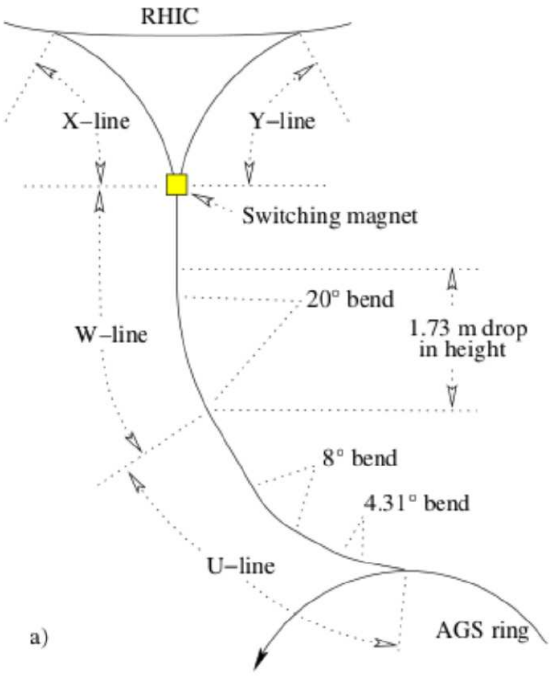

Figure 1: The AtR line.

Details regarding the AGS to RHIC transport line, geometry, spin considerations, coordinate system, etc., can be found in Ref. [2]. A treatment of the AGS to RHIC spin matching can be found in an earlier works, Refs. [3, 4]. On the other hand, in order to allow answering possible questions regarding details of the geometry and optics of the AtR model in Zgoubi, and also in order to facilitate further checks or investigations, the Zgoubi I/O data files relating to the present work have been archived in dedicated folders in

$$/rap/lattice\_tools/zgoubi/AgsZgoubiModel/AtR/n0$$

from where they can be copied and run using the on-line Zgoubi executable. Various aspects of the computing tools and methods employed in the present study will be discussed in due place in the sequel in that aim.

The present investigations use newly computed 3-D OPERA maps of the AGS cold snake, including a new setting of the cold snake solenoid [1], together with the machinery of the AGS model developed in the stepwise ray-tracing code Zgoubi [5, 6]. These new OPERA field maps of the cold snake are archived in

$$/rap/lattice\_tools/zgoubi/AgsZgoubiModel/snakeFieldMaps/coldSnake/RGFiles$$

[1] AGS and RHIC planes differ in height by 1.73 m.

[2] The two helical partial snakes in the AGS cause a tilt of the stable spin direction away from the vertical.

[3] Due to the partial snakes in the AGS and to the vertical bends in the AtR, spin matching from AGS to RHIC can not be perfect.

The warm snake OPERA maps are archived in

$$/rap/lattice\_tools/zgoubi/AgsZgoubiModel/snakeFieldMaps/warmSnake/$$

Users can find guidance in the "README" files included in these folders.

Table 1: Characteristics of the warm and cold snakes.

		Warm snake$^{(a)}$	**Cold snake**$^{(c)}$	
		set/meas./OP$^{(b)}$		
Helix coil current	A	2670/2635/2540	238.7	238
(relative to 350 Amp)	*%*	-	*(68.2)*	*(68)*
Solenoid current	A	-	148	76
(relative to 350 Amp)	*%*	-	*(42.3)*	*(21.6)*
Snake strength, $G\gamma\ : 4.5 \rightarrow 45.5$	%	6.69 $\rightarrow$ 5.87	14.71 $\rightarrow$ 10.59	13.25 $\rightarrow$ 10.40
$\vert\vec{B}\vert$ at helix center, B_{00}	T	1.5309	2.173	2.163
$\int_{\text{axis}} \vert\vec{B}(z)\vert\, dz$	T.m	3.2276	4.353	4.327
Straight mag. $\mathcal{L} = \frac{\int_{\text{axis}} \vert\vec{B}\vert\, dz}{B_{00}}$	m	2.108	2.004	2.000
Max. $\vert\vec{B}(s)\vert$ on orbits, $G\gamma\ :\ 4.5 \rightarrow 45.5$	T	1.5333 $\rightarrow$ 1.5309	2.171 $\rightarrow$ 2.183	2.164 $\rightarrow$ 2.163
$\int_{\text{orbit}} B_z(s)\, ds$, $G\gamma\ :\ 4.5 \rightarrow 45.5$	T.m	-0.16 $\rightarrow$ -0.014	-0.03 $\rightarrow$ +0.23 (0 at $G\gamma \approx 5.2$)	-0.15 $\rightarrow$ +0.11 (0 at $G\gamma \approx 9$)
Orbit radius , $G\gamma\ : 4.5 \rightarrow 45.5$	mm	19.2 $\rightarrow$ 1.6	23.6 $\rightarrow$ 2.1	23.3 $\rightarrow$ 2.1
Spin prec. ϕ, $G\gamma\ : 4.5 \rightarrow 45.5$	deg	12.04 $\rightarrow$ 10.56	26.47 $\rightarrow$ 19.07	23.86 $\rightarrow$ 18.73

(a) Map name : "table55.tab", as used in Zgoubi input data files.
(b) Case 2670 A : current set in AGS controls for 1.53 T field on plateau. Case 2635 A : measured current with the former setting. Case 2540 A : theoretical value in OPERA, using the "perfect model" of the snake (i.e., the model of the magnet free of deformation [7]) yielding 1.53 T on the plateau.
(c) A linear combination of the following two 3-D OPERA field maps [1] :
- "ags-full-coilv5-x06-rerun2-x071-sol-152a-nodal-x5y5z10mm.table",
- "ags-helical-solenoid-april2013-coilv5-x071-sol-81_2A-integral-x5y5z10mm.table".

2 Snake hypotheses

The $G\gamma$ region of interest regarding the snake parameters is that of the optimum extraction and transport of the spin $\vec{n}_0$ vector to RHIC, namely $45 \leq G\gamma \leq 49$ about.

• **Warm snake :** The field map "table.55.map" is used. The main properties drawn from it are recalled in Tab. 1, col. .3 (more details in Ref. [1]).

The spin precession along the AGS cycle can be interpolated using, see Fig. 2,

$$\mu(B, G\gamma)[deg.] = (B/B_0)^2 \left[C_0 + C_1/G\gamma + C_2/(G\gamma)^2\right] \quad (1)$$

with B the field plateau along the orbit, in the vicinity of $B_0 = 1.5333$ Tesla

and $\quad C_0 = 10.578,\ C_1 = -1.284,\ C_2 = 34.60$

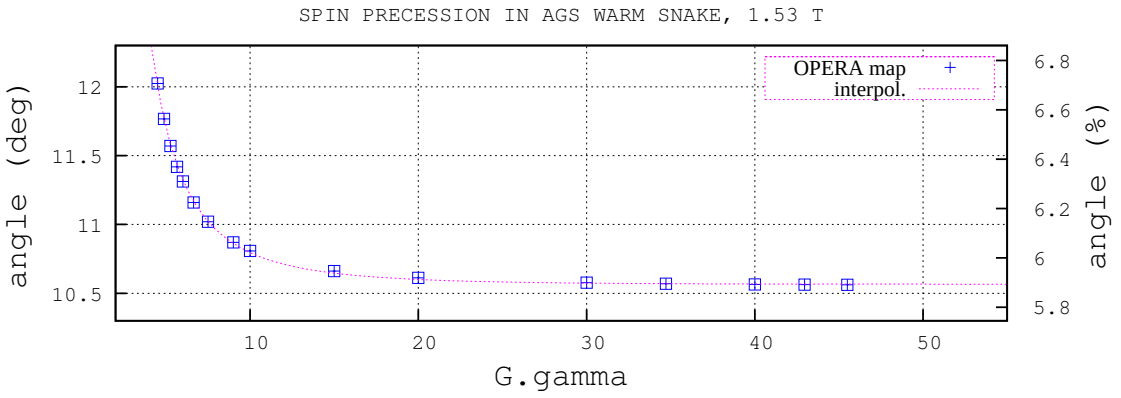

Figure 2: Spin precession angle in the warm snake, at various $G\gamma$ values, and interpolation function Eq. 1.

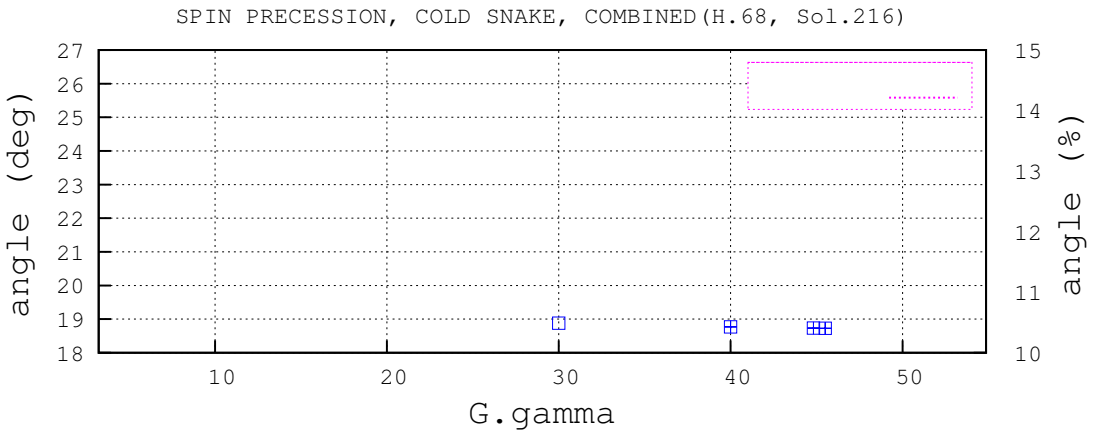

Figure 3: Spin precession angle in the cold snake, 68% helix and 76 Amp solenoid current, at various $G\gamma$ values, and interpolation function Eq. 2.

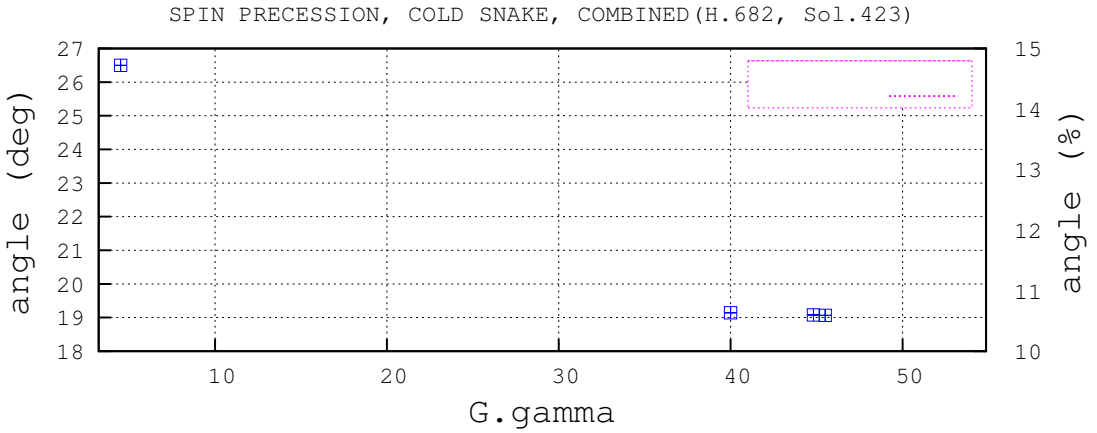

Figure 4: Spin precession angle in the cold snake, 68.2% helix and 148 Amp solenoid current, at various $G\gamma$ values, and interpolation function Eq. 3.

• **Cold snake :** The field map used is obtained by combining independently computed, 3-D OPERA, helix and solenoid field maps, as follows, *cf.* Tab. 1 (details in Ref. [1]).

(i) In the case of the nominal setting, 68% helix (238 Amp) and 21.6 % solenoid (76 Amp) so to cancel $\int B_s\, ds$, rightmost column in Tab. 1, the combination is

$$1.016 \times [\ 0.9577 \times \text{ags-full-coilv5-x06-rerun2-x071-integral-x5y5z10mm.table} \\ \oplus 0.216 \times \text{ags-full-sold3-only-nodal-x5y5z10mm-wasactually-integral.table}\ ]$$

with '"1.016" an empirical factor ensuring same spin precession as a complete, single, helix+solenoid OPERA map, this is discussed in Ref. [1].

The spin precession along the AGS cycle can be interpolated using, see Fig. 3,

$$\mu(B, G\gamma)[deg.] = (B/B_0)^2\ \left[C_0 + C_1/G\gamma + C_2/(G\gamma)^2\right] \tag{2}$$

with B the field plateau along the orbit, in the vicinity of $B_0 = 2.163$ Tesla

and $C_0 = 18.4937,\ C_1 = 9.5128,\ C_2 = 61.5222$

(ii) In the case of 68.2% helix (238.7 Amp) and 42.3 % solenoid (148 Amp), column 4 in Tab. 1, the combination is

$$1.016 \times [\ 0.9606 \times \text{ags-full-coilv5-x06-rerun2-x071-integral-x5y5z10mm.table} \\ \oplus 0.423 \times \text{ags-full-sold3-only-nodal-x5y5z10mm-wasactually-integral.table}\ ]$$

Eq. 2 in this case becomes, Fig. 4

$$\mu(B, G\gamma)[deg.] = (B/B_0)^2\ \left[C_0 + C_1/G\gamma + C_2/(G\gamma)^2\right] \tag{3}$$

with B the field plateau along the orbit, in the vicinity of $B_0 = 2.173$ Tesla

and $C_0 = 18.6092,\ C_1 = 19.6655,\ C_2 = 66.0743$

Table 2: AGS parameters, in presence of G09 and H11 bumps designed with six bump dipoles each, G10 kicker off, and with orbit orbit bump compensation at both snakes.

γG		45.5
Closed orbit length	(m)	807.1006$^{(a)}$ 807.091$^{(b)}$
Rigidity	(T.m)	79.2855
Qx, Qy		[8].7251, [8].9093
Q'x, Q'y		-7.66, +1.13
$\alpha, \gamma_{\rm tr}$		0.01382, 8.5064
Periodic functions at entrance to "A01BF" :		
$\beta_x,\ \beta_y$	(m)	21.85, 10.81
$\alpha_x,\ \alpha_y$		-1.66, +0.95
D_x, D'_x	(m,-)	-2.588, -0.145
D_y, D'_y	(m,-)	+0.002, -0.0007

(a) Extraction bumps G09-H11 set (see Fig. 5).
(b) Extraction bumps G09-H11 off, no snakes.

3 AGS ring, periodic $\vec{n}_0$ at H10

The setting considered in the following is the nominal one, 68% helix (238 Amp), 21.6% solenoid (76 Amp).

3.1 AGS settings, G09 and H11 bumps

An AGS template data file suitable for the present study can be found in the AgsZgoubiModel repository, namely

/rap/lattice_tools/zgoubi/AgsZgoubiModel/templateZgoubi4ZgoubiFromSnaprampCmd_library/
ppmUser4_pp/templateZgoubi4ZgoubiFromSnaprampCmd.dat

It has been tuned here, to regular extraction optics conditions, as listed in Tab. 2. It includes orbit compensation at both snakes, as well as the local "G09" and "H11" extraction bumps. The "G09 bump" positions the orbit at G10 kicker, the "H11 bump" positions the orbit at H10 extraction septum. Note that these two bumps are horizontally

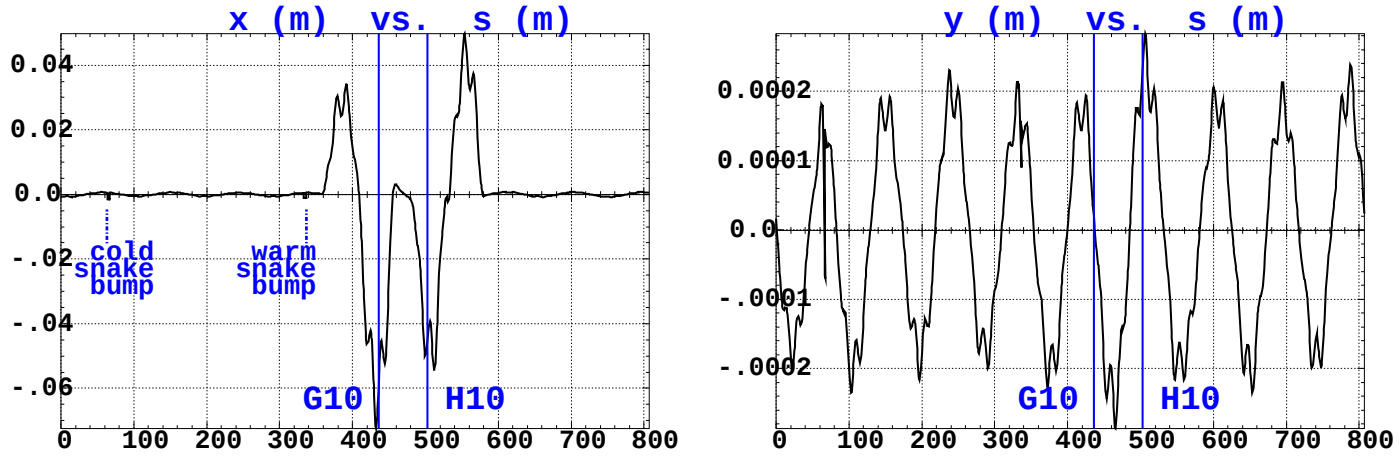

Figure 5: Residual orbit along the AGS ring in presence of G09 and H11 bumps tuned for extraction, AGS settings as in Tab. 2. G10 kicker is off, here. Left : horizontal orbit, right : vertical orbit. The two snake bumps are still visible, very small at that rigidity.

well closed, Fig. 5-left, by using an independent power supply for each one of the six dipole back-leg windings in a bump (respectively, F08CD, F09BF, G02BF, G03CD, G16AD, G17CF for G09 and H04CD, H05AF, H18CF, H19BD, I12BD, I13CF for H11) whereas in real life only two power supplies are used, one per series, so yielding some residual horizontal orbit. A $\pm$0.3 mm vertical orbit remains, induced by the snakes, of marginal effect in the present study. This is a deliberate choice to work out these simulations with a quasi-zero orbit, possible differences in the orientation of the local $\vec{n}_0$ at the extraction septum H10, compared to real-life orbit, remain to be studied.

3.2 Finding $\vec{n}_0$

The local $\vec{n}_0$ at arbitrary location around the AGS ring can be found using the "FIT" procedure in Zgoubi, the constraint being : identical coordinates of the spin, at start and after one ring turn, for a particle on the closed orbit. This AGS ring sequence in Zgoubi has to be completed with the "FIT" instructions for that. The input data excerpts, appendix B, show the start of the sequence and the additional instruction that complete it for $\vec{n}_0$ search.

In a second step, once the periodic $\vec{n}_0$ has been found, that file has to be added the optical element sequence that leads from its current downstream end (in the present case, the downstream end of L20 drift, entrance to A01BF) to the H10 extraction septum, via the G10 extraction kicker, this is discussed in the next section.

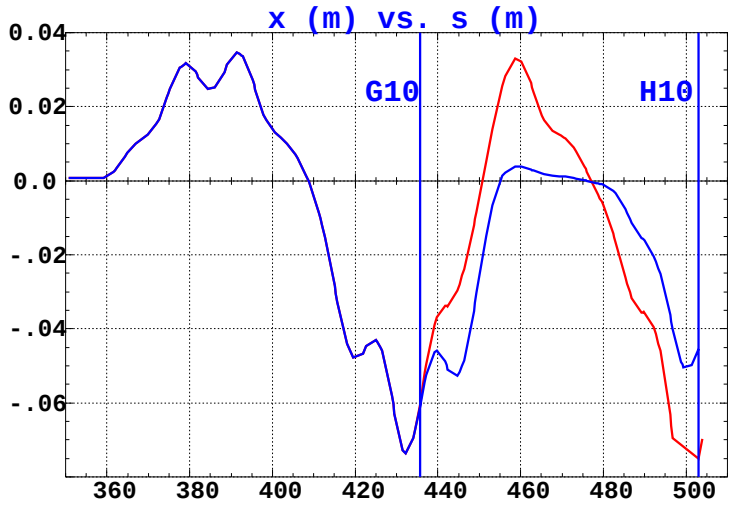

Figure 6: A zoom on the extraction bump region, down to H10. Blue : G10 kick off, red : G10 kick on.

3.3 Transporting $\vec{n}_0$ to H10

The periodic $\vec{n}_0$ on the closed orbit in the AGS is first determined, using the procedure described in the previous section, in the presence of the G09, H11 extraction bumps and in the absence of kick at G10. Then $\vec{n}_0$ is transported to the region of the extraction septum H10, Fig. 6. In a second step G10 is fired, so displacing the orbit all the way down to the H10 septum extraction channel, the red path in Fig. 6.

Table 3: Use of the 'SYSTEM' and " 'SPNPRT' PRINT" commands in a $G\gamma$ scan.

```
Template zgoubi.dat. 2 snakes.
 'OBJET'
79.2855199D3            Beam rigidity : the quantity to be varied
2
1 1
0. 0. 0. 0. 0. 1. 'o'
1

 'SPNTRK'              3
4.1
0. 0. 1.

 'SCALING'   LBL_SCLfit7                    Power supply commands
1   14
AGSMM *AF *BF *CF  ! dB0 (FIT#3),   dB1 (FIT#4),    dB2
-1          3        13   1.        14    4e-20     15   5.E-20
1.000000006    ! (FIT #6)
1
.................................
......... AGS RING    ............
.................................
.................................
..... A01BF-H10MID SECTION  .......
... INCLUDING BUMP & G10 kick .....
.................................
```

```
 'AGSMM'     MM_H10BF                                    AGS main magnet
0
3 0 0   0.  1.00000E+00  1.00000E+00
2  1 0.  1 0.
0. 0. 10.00  4.0  0.800 0.00 0.00 0.00 0.00 0. 0. 0. 0.
4  .1455   2.2670  -.6395  1.1558  0. 0.  0.
0. 0. 10.00  4.0  0.800 0.00 0.00 0.00 0.00 0. 0. 0. 0.
4  .1455   2.2670  -.6395  1.1558  0. 0.  0.
0. 0. 0. 0. 0. 0. 0. 0. 0. 0.
10.0  Dip MM_H10BF
3    0.0 -0.3942767 0.011751150                  angle =  -0.0235023 rad
 'DRIFT'     D10
152.3839
 'MARKER'    H10MID
 'FAISCEAU'
 'SPNPRT' PRINT                    Will store spin in zgoubi.SPNPRT.out

 'SYSTEM'            Allows checking bumps in whole Ggamma scanned range
  1
  cat zgoubi.fai >> catOrbits.data

 'END'
```

3.4 Checking the orbit down to H10, while scanning $G\gamma$: $42 \rightarrow 50$

Once the AGS periodic orbit is settled for a particular $G\gamma$, the scaling of the ring optics with energy (a function which is ensured by the "SCALING" power supply procedure in Zgoubi, appendix B) can be monitored, see Fig. 7, to make sure that possible residual orbit excursions during the scan remain small.

The problem in Tab. 3 (an excerpt of Zgoubi input data list of page 21) is repeated over the set of $G\gamma$ values of interest in that aim. The final "SYSTEM" command in the data list stores the orbits and their $\vec{n}_0$ in a dedicated file, "catOrbits.data", for further plot, see Fig. 7.

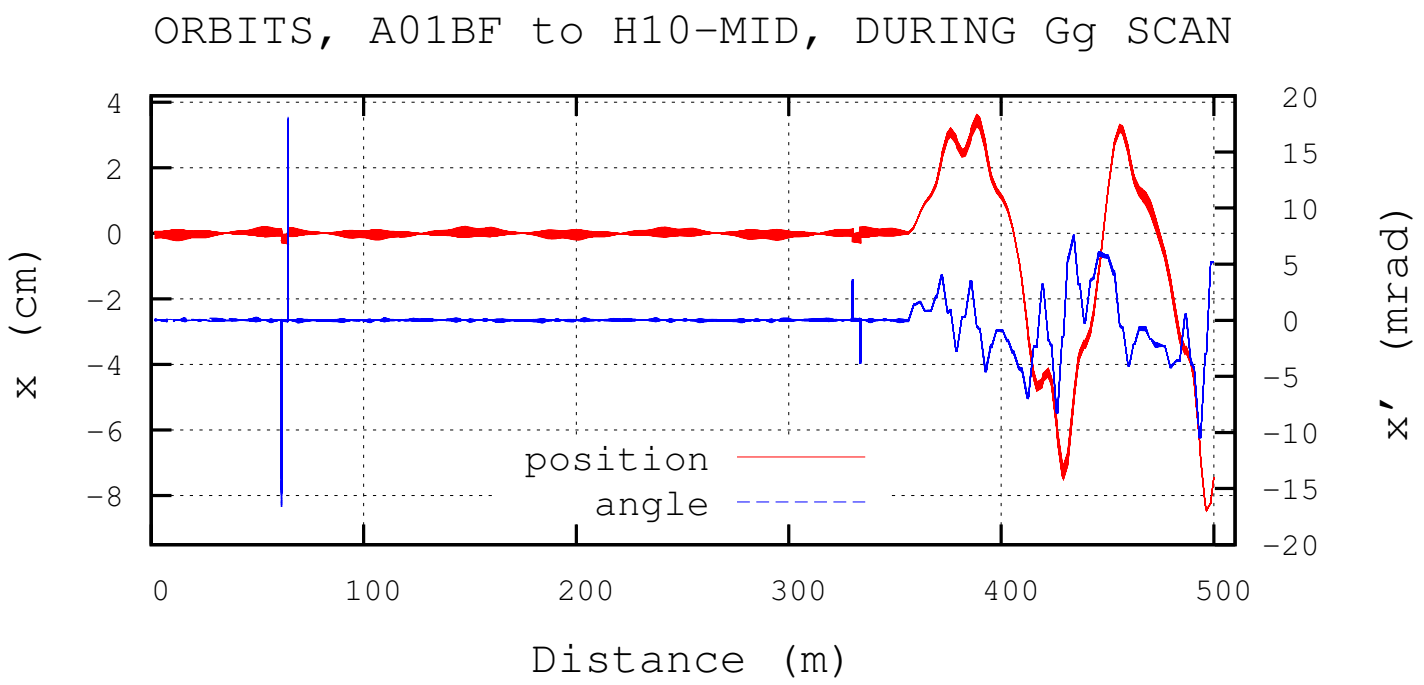

Figure 7: For about 30 different values of $G\gamma \in [42, 50]$, superimposed orbits ("x", left axis, red curves) and their derivatives ("x' ", right axis, blue curves), from A01BF AGS main magnet to the center of the H10 extraction septum straight section. The horizontal axis is the distance along the orbit. G10 kicker is "on", orbit position at H10 is -75 mm, angle about +50mrd.

It can then be observed, Fig. 7, that the orbit is not perfectly cancelled, it sweeps over a small x interval when $G\gamma$ changes, however with marginal maximum excursion whatever $G\gamma$, and with marginal effect on $\vec{n}_0$ which is the relevant criterion.

4 AtR

4.1 Zgoubi model

A model of the AtR line in Zgoubi has been obtained by translation from MAD8 data files. It covers from UBEGIN to RHIC kicker (Fig. 1),

- then H10 septum is added,

- as well as H11, H12 and H13 AGS main magnet wakes, which the extracted path downstream of the septum does cross. They are simulated in a simplified way that takes care simply of the orbit, namely, with reduced-field H11BD (11.85 mrad), H12BD (6.18 mrad), H13CF (3.67 mrad).

The AtR (Fig. 1) is organized as follows, see Fig. 1 :

- the UBEGIN to W-End section is common to both Blue and Yellow injections,

- then the "switching magnet" follows and, by a change in field sign, directs the beam towards either the X (RHIC-Blue) or Y (RHIC-Yellow) branch.

- The X and Y lines differ essentially by the sign of the angle in the bends, and by the particular settings of the injection path along RHIC arcs, Blue and Yellow respectively.

That model of the AtR in Zgoubi, as well as the various files used for checking transport matrices against MAD8, checking the orbits along the AtR, etc., have been archived in

$$/rap/lattice\_tools/zgoubi/AgsZgoubiModel/AtR/n0$$

Additional informations regarding general AtR geometrical data can be found in Ref. [2].

4.2 Transport matrices, from H10 to RHIC kickers

Transport matrices from both MAD8 and Zgoubi are displayed here, for comparison. The non-zero anti-diagonal blocks arise from the presence of skew optics along the line, including dipoles, RHIC ring being lower in elevation than AGS ring.

From H10 to RHIC-Blue kicker :

```
MAD8

   Length: 581.026
      -2.796068       17.367812       -0.016389       -0.033368        0.000000       -1.065488
      -0.039314       -0.113439       -0.000903       -0.003215        0.000000       -0.024004
       0.010052       -0.107989        1.184843       10.183856        0.000000        0.020349
       0.000160        0.000523       -0.168178       -0.601530        0.000000        0.003584
      -0.025262        0.538168       -0.007100       -0.046116        1.000000       -2.822765
       0.000000        0.000000        0.000000        0.000000        0.000000        1.000000

ZGOUBI

   length :   581.02556
      -2.78658         17.2839       -1.637868E-02   -3.346093E-02     0.00000        -1.06058
     -3.943741E-02   -0.114243       -9.066873E-04   -3.230374E-03     0.00000       -2.423199E-02
      1.007545E-02   -0.108164         1.18162         10.1841         0.00000        2.033039E-02
      1.593392E-04    5.295908E-04   -0.167967       -0.601396         0.00000        3.588438E-03
      2.573239E-02   -0.540403        7.090202E-03    4.615573E-02     1.00000         2.82454
       0.00000         0.00000         0.00000         0.00000         0.00000         1.00000
```

From H10 to RHIC-Yellow kicker :

```
MAD8

    length  581.026
      -2.796068       17.367809       -0.016356       -0.033083        0.000000       -2.731881
      -0.039314       -0.113439       -0.000908       -0.003232        0.000000       -0.122564
       0.010130       -0.108475        1.184844       10.183857        0.000000        0.020402
       0.000161        0.000527       -0.168178       -0.601530        0.000000        0.003586
      -0.235330        2.438970       -0.007205       -0.044019        1.000000       -2.887779
       0.000000        0.000000        0.000000        0.000000        0.000000        1.000000

ZGOUBI

   length : 581.02556
      -2.78519         17.2776       -1.635967E-02   -3.323377E-02     0.00000        -2.75769
     -3.962287E-02   -0.113239       -9.122731E-04   -3.249350E-03     0.00000       -0.120813
      1.013991E-02   -0.108550         1.17502         10.1585         0.00000        7.334280E-03
      1.606287E-04    5.329169E-04   -0.168038       -0.601729         0.00000        3.987950E-04
      0.227223        -2.39969        1.161749E-03    3.518871E-03     1.00000         2.90837
       0.00000         0.00000         0.00000         0.00000         0.00000         1.00000
```

4.3 Checking orbits along UWX, UWY

Once the AtR Zgoubi files for RHIC-Blue and RHIC-Yellow injections are settled, the orbits along the AtR, over the all $G\gamma \ : 42 \rightarrow 50$ range scanned, need be checked (in a similar manner to the AGS orbits, Fig. 7) so to make sure they remain small enough at all $G\gamma$. Fig. 8 summarizes these data at the downstream end of the X and Y lines, showing that the orbits end up with quasi-zero angles and horizontal positioning at RHIC kickers, and vertical position in millimeter range in the present simulation.

The two discontinuities in the x orbit ($s = 259$ m and 274 m), Fig. 8, are artefacts resulting from rotations of the local frame. Same effects for y, $s = 300$ m region. The discontinuity in y at $s = 283$ m stems from a vertical change of frame to RHIC level, $\delta y = 2.5$ cm, placed at the location where the AtR line meets RHIC arc quadrupole.

BLUE

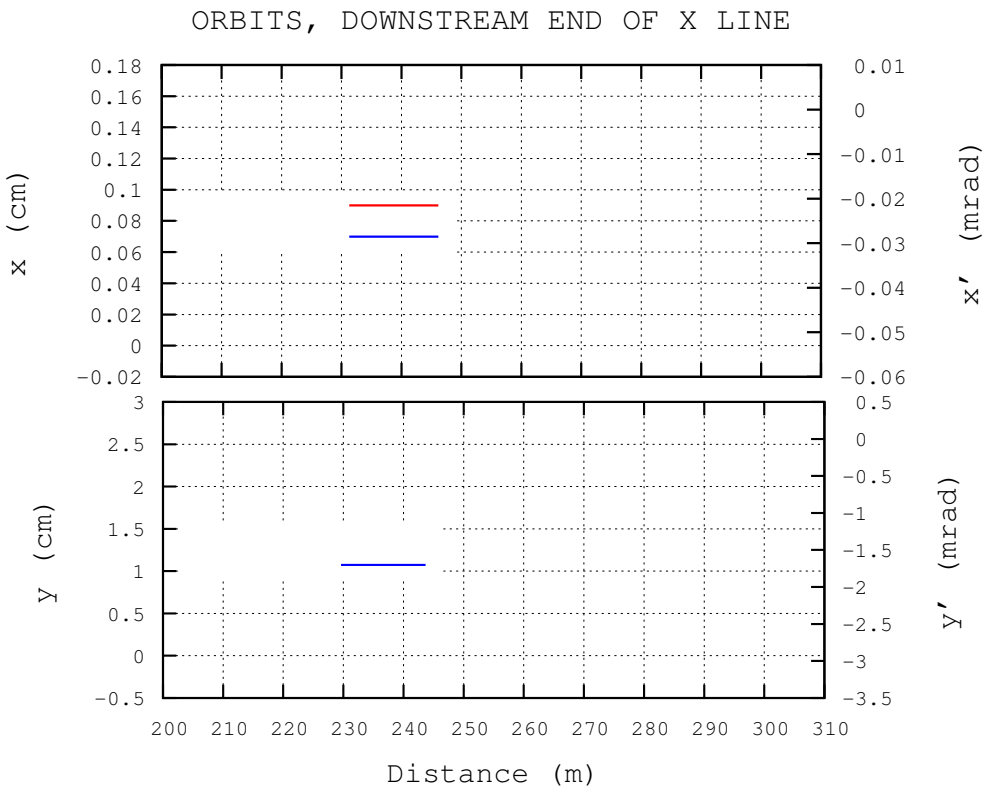

YELLOW

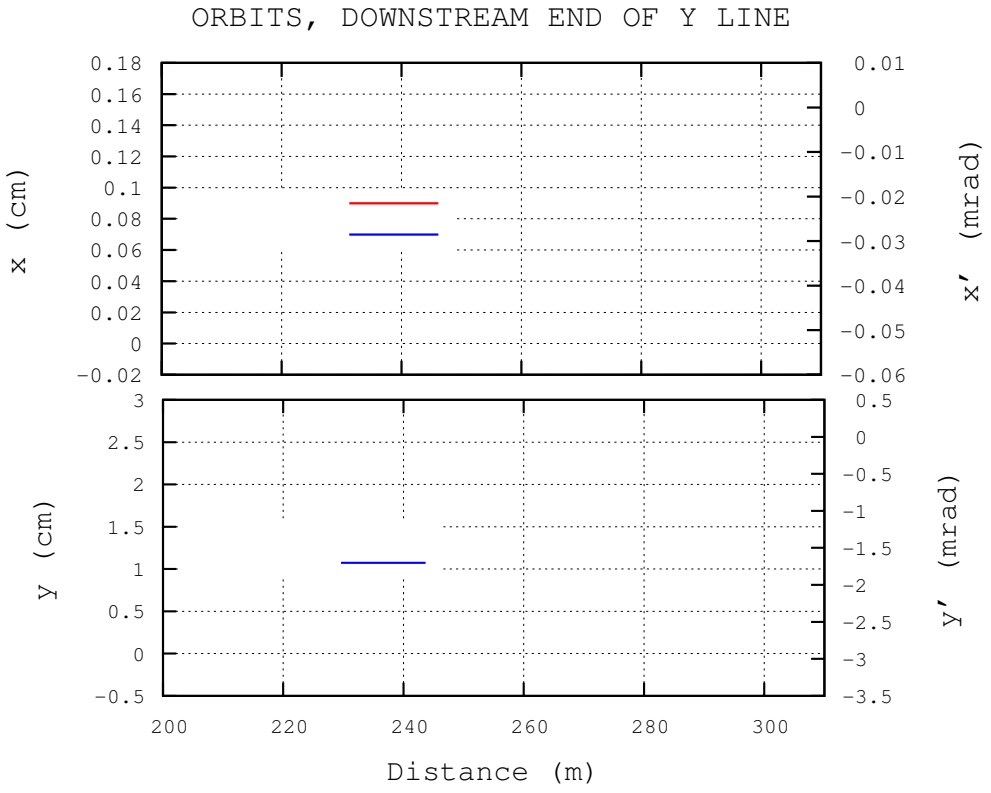

Figure 8: Orbits and derivatives in RHIC Blue and Yellow kicker regions.

5 $\vec{n}_0$ transmission, from H10 to RHIC kickers

The optics settings and the orbits discussed in the previous sections are now accounted for, including

- the dipole effect of the wakes at the H10, H11 and H13 AGS main magnets,
- the "G09 bump" (extraction kicker) and the "H11 bump" (septum),
- with G10 kicker off when determining the periodic $\vec{n}_0$ in the AGS,
- the orbit deviation by the G10 kicker when determining $\vec{n}_0$ at the start of the AtR line.

A scan of $G\gamma$ in the range $[42, 50]$ then yields the plots in Fig. 9 in the two different cases of helix and solenoid strengths. The figure shows the vertical projection of the $\vec{n}_0$ vector at three different locations : H10 septum in the AGS after extraction by G10 kicker, RHIC-Blue kicker, RHIC-Yellow kicker. The optimum extraction $G\gamma$ can be determined from the scan : it has to be close to a half-integer value, and such that the vertical projection of the $\vec{n}_0$ is closest to 1 at the injection kicker at the downstream end of the X line (RHIC Blue ring) and of the Y line (RHIC Yellow). Detailed numerical values of $\vec{n}_0$ components at H10 and at RHIC kickers, for half-integer $G\gamma$ in $[43.5, 49.5]$, are given on page 15 (case of 68% helix, 76 Amp solenoid) and page 16 (case of 68.2% helix, 148 Amp solenoid).

For comparison, Fig. 10 shows the results obtained using spinor algebra. All dipole components met along the AtR, as well as the skewing of the non-planar orbit, are accounted for. The agreement between the two methods, stepwise ray-tracing and spinors, seems sufficient that the optimum extraction $G\gamma$ value can be inferred from either one. However the fine structure in the orientation of $\vec{n}_0$ at RHIC kickers may show % scale discrepancies for some regions in the $G\gamma$ scan.

Fig. 10-bottom also displays data from Ref. [2], for comparison. They were obtained for a stronger cold snake, 15 %. This shows that the level of sensitivity of the orientation of $\vec{n}_0$ at RHIC kickers to the snake strength can be in the % range, depending on the $G\gamma$ region.

Case cold snake 68.0% (238.0 Amp) with solenoid 21.6% (76 Amp). Warm snake 1.53 Tesla.

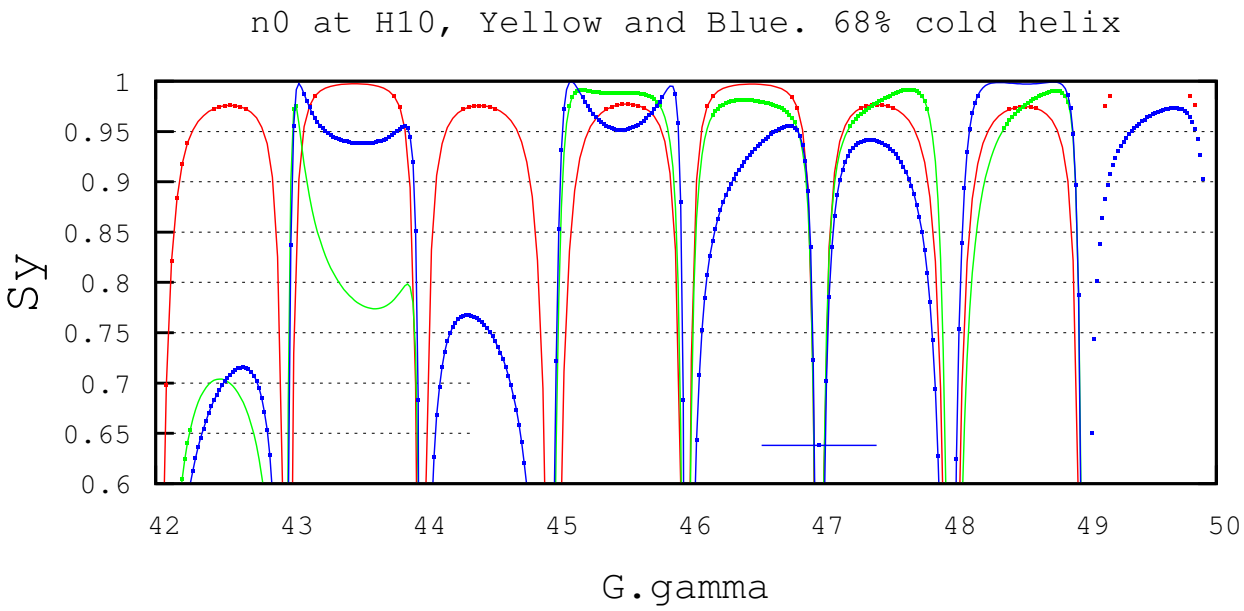

Case cold snake 68.2% (238.7 Amp) with solenoid 42.3% (148 Amp). Warm snake 1.53 Tesla.

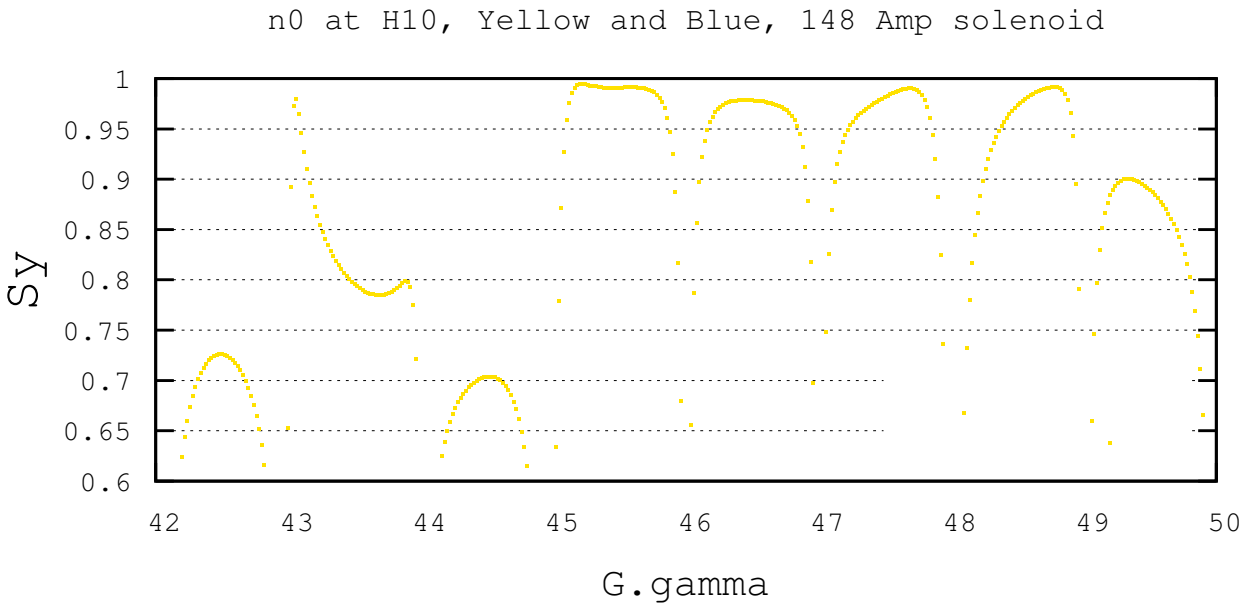

Figure 9: A scan of the transmission of $\vec{n}_0$ through the AtR, from AGS H10 extraction septum to the downstream end of RHIC kickers, for $G\gamma \in [42, 50]$. The vertical axis gives the modulus of the projection of the $\vec{n}_0$ vector on the vertical, at the three different locations, H10 and the RHIC Blue and Yellow kickers.

Spinor algebra, warm snake 5.9%, cold snake 10.3%

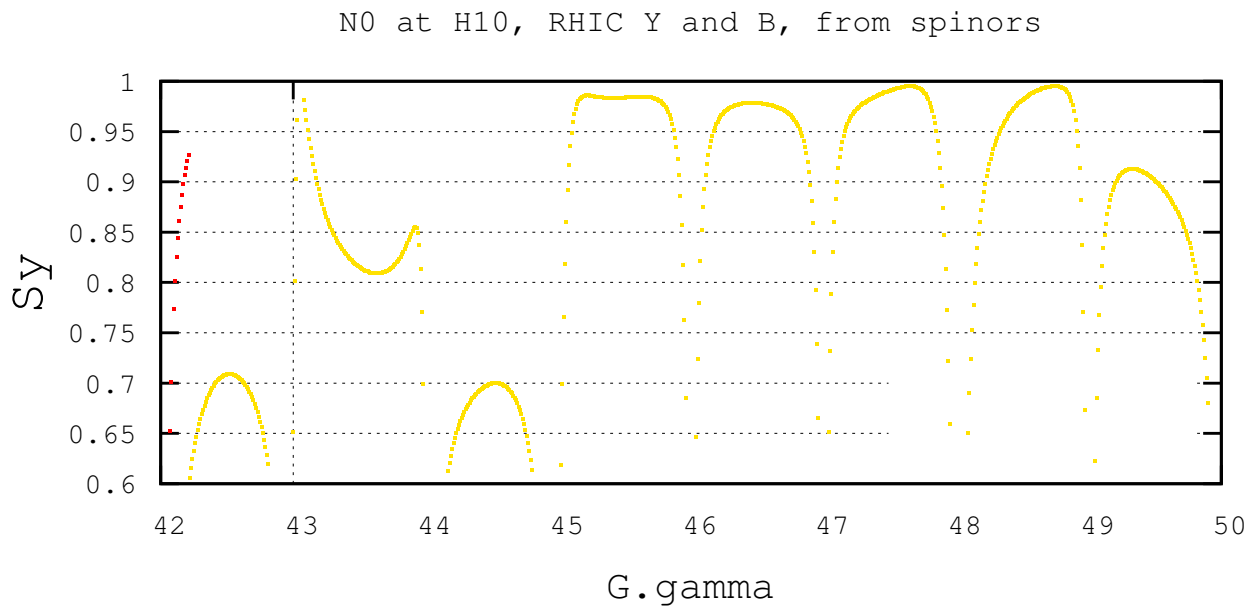

EPAC 2006 paper - Warm snake 5.9%, cold snake 15%

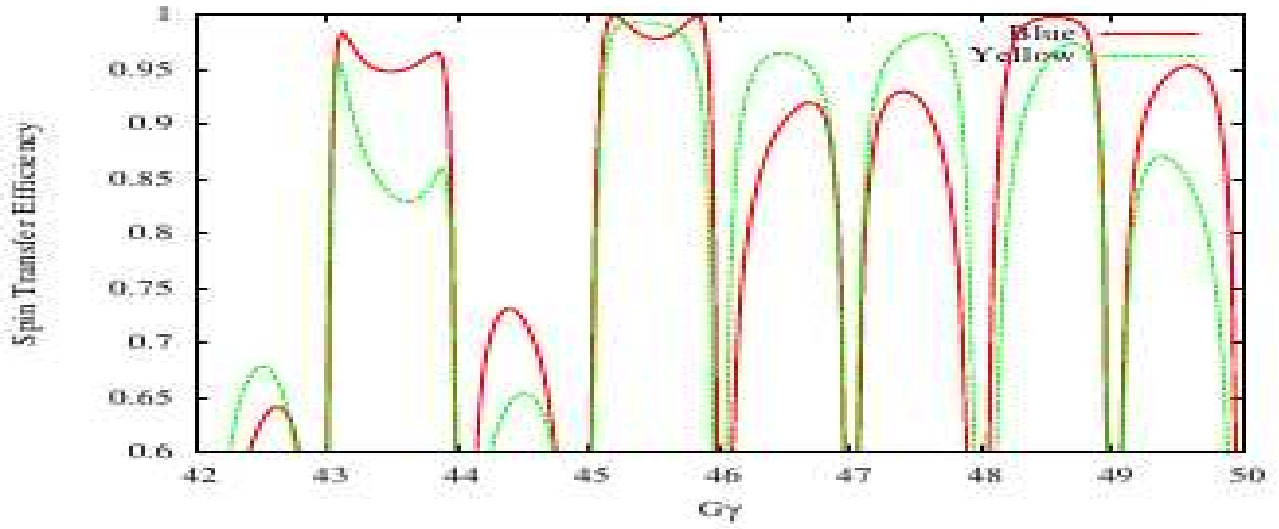

Figure 10: For comparison with Fig. 9, top plot : using spinor algebra, bottom plot : an earlier simulation [2] accounting for 5.9 % warm snake and 15 % cold snake.

• Detailed values of the spin $\vec{n}_0$ vector components at H10 and RHIC kickers (cols. 5-7), for half-integer values of $G\gamma$ taken between 43.5 and 49.5 (rightmost column).

Snake conditions : cold helix 68.0% (equivalent to 238.0 Amp), solenoid 0.216 (equivalent to 76 Amp), warm helix 1.53 Tesla.

Series of 3 lines in the table below : respectively, downwards, H10/Blue kicker/Yellow kicker.

#---------- n0 At A01BF ----------				|---- n0 At H10/Blue/Yellow kickers (lines 1/2/3 resp.) ---					
# Sl	Sx	Sz	|S|	Sl	Sx	Sz	|S|	gamma	G.gamma
4.990398E-02	4.902606E-02	9.975309E-01	9.999809E-01	-2.113578E-02	-6.860254E-02	9.974202E-01	1.000000E+00	2.426308E+01	4.350000E+01
				-2.257319E-01	-2.606375E-01	9.386763E-01	1.000000E+00		
				6.229318E-01	7.460126E-03	7.822406E-01	1.000000E+00		
1.811797E-01	1.240055E-01	9.756379E-01	1.000036E+00	-7.530302E-02	2.084171E-01	9.751368E-01	1.000000E+00	2.482085E+01	4.450000E+01
				5.882251E-01	-2.918372E-01	7.542031E-01	1.000000E+00		
				3.891089E-01	-6.077095E-01	6.923030E-01	1.000000E+00		
1.806584E-01	-1.277366E-01	9.751989E-01	9.999835E-01	-3.378445E-02	-2.125238E-01	9.765717E-01	1.000000E+00	2.537862E+01	4.550000E+01
				2.532695E-01	1.745843E-01	9.515119E-01	1.000000E+00		
				3.491268E-02	-1.476747E-01	9.884196E-01	1.000000E+00		
5.319616E-02	-5.097394E-02	9.972840E-01	1.000002E+00	-3.531638E-02	6.768758E-02	9.970813E-01	1.000000E+00	2.593640E+01	4.650000E+01
				6.968758E-02	3.621176E-01	9.295238E-01	1.000000E+00		
				9.637766E-02	1.697123E-01	9.807696E-01	1.000000E+00		
1.294925E-01	-1.814266E-01	9.748971E-01	1.000054E+00	1.920710E-01	-1.044964E-01	9.758018E-01	1.000000E+00	2.649417E+01	4.750000E+01
				3.059217E-01	1.680534E-01	9.371072E-01	1.000000E+00		
				2.930384E-02	-1.809897E-01	9.830483E-01	1.000000E+00		
-1.281207E-01	-1.857064E-01	9.741564E-01	9.999412E-01	-1.274183E-01	1.858462E-01	9.742822E-01	1.000000E+00	2.705194E+01	4.850000E+01
				7.002172E-02	9.537915E-03	9.974999E-01	1.000000E+00		
				9.333645E-02	-2.246846E-01	9.699511E-01	1.000000E+00		
-4.713306E-02	-5.467764E-02	9.973663E-01	9.999753E-01	6.090476E-02	-2.513392E-02	9.978271E-01	1.000000E+00	2.760971E+01	4.950000E+01
				-8.605678E-02	2.460049E-01	9.654407E-01	1.000000E+00		
				4.652116E-01	-1.232612E-01	8.765756E-01	1.000000E+00		

• Detailed values of the spin $\vec{n}_0$ vector components at H10 and RHIC kickers (cols. 5-7), for half-integer values of $G\gamma$ taken between 43.5 and 49.5 (rightmost column).

Snake conditions : cold helix 68.2% (equivalent to 238.7 Amp), solenoid 0.423 (equivalent to 148 Amp), warm helix 1.53 Tesla.

Series of 3 lines in the table below : respectively, downwards, H10/Blue kicker/Yellow kicker.

#---------- n0 At A01BF ----------				|---- n0 At H10/Blue/Yellow kickers (lines 1/2/3 resp.) ---					
# Sl	Sx	Sz	|S|	Sl	Sx	Sz	|S|	gamma	G.gamma
4.732510E-02	4.806584E-02	9.976955E-01	9.999731E-01	-1.814651E-02	-6.497543E-02	9.977219E-01	1.000000E+00	2.426308E+01	4.350000E+01
				-2.582524E-01	-2.490897E-01	9.334131E-01	1.000000E+00		
				6.059603E-01	-9.718531E-03	7.954355E-01	1.000000E+00		
1.767078E-01	1.287243E-01	9.758025E-01	9.999930E-01	-7.045743E-02	2.072110E-01	9.757558E-01	1.000000E+00	2.482085E+01	4.450000E+01
				5.656136E-01	-3.051170E-01	7.661493E-01	1.000000E+00		
				3.621251E-01	-6.135094E-01	7.017632E-01	1.000000E+00		
1.759671E-01	-1.288889E-01	9.759671E-01	1.000044E+00	-3.587773E-02	-2.148070E-01	9.759973E-01	1.000000E+00	2.537862E+01	4.550000E+01
				2.518196E-01	1.636654E-01	9.538346E-01	1.000000E+00		
				1.712980E-02	-1.345443E-01	9.907595E-01	1.000000E+00		
4.781893E-02	-4.740741E-02	9.976955E-01	9.999652E-01	-3.037510E-02	6.007709E-02	9.977315E-01	1.000000E+00	2.593640E+01	4.650000E+01
				7.710535E-02	3.662662E-01	9.273100E-01	1.000000E+00		
				1.043053E-01	1.750519E-01	9.790185E-01	1.000000E+00		
1.281207E-01	-1.769822E-01	9.758299E-01	9.999908E-01	1.910362E-01	-1.072492E-01	9.757063E-01	1.000000E+00	2.649417E+01	4.750000E+01
				2.855551E-01	1.810073E-01	9.411135E-01	1.000000E+00		
				3.011611E-02	-1.925855E-01	9.808180E-01	1.000000E+00		
-1.295473E-01	-1.753086E-01	9.759671E-01	1.000014E+00	-1.161197E-01	1.835693E-01	9.761242E-01	1.000000E+00	2.705194E+01	4.850000E+01
				3.630951E-02	9.751598E-03	9.992930E-01	1.000000E+00		
				5.961301E-02	-2.236810E-01	9.728376E-01	1.000000E+00		
-4.757202E-02	-4.748971E-02	9.977778E-01	1.000039E+00	6.305058E-02	-2.348125E-02	9.977341E-01	1.000000E+00	2.760971E+01	4.950000E+01
				-9.410003E-02	2.181134E-01	9.713762E-01	1.000000E+00		
				4.478883E-01	-9.821203E-02	8.886791E-01	1.000000E+00		

6 Conclusion

According to the latest cold snake field maps generated by R. Gupta, we have been using a solenoid field twice as strong as needed for many years. This setting does not minimize the coupling when crossing the $0 + Q_y$ spin resonance.

This paper analyzed the impact of the change of the solenoid field on the stable spin direction at AGS extraction and RHIC injection. In addition, a more careful analysis at AGS extraction with fringe field from the main magnets considered, has also been done. The results show that the impact on the vertical components at RHIC injection is small.

Besides the main plots, data files are also listed for various $G\gamma$ values and solenoid strengths. Last but not the least, the spin rotation angles for various snake combinations have also been calculated and empirical fitting formulas are given. For the future calculation, these are the best estimation of stable spin direction and snake strength and should overwrite the past publications.

APPENDIX

A Transport matrices, MAD and Zgoubi

Obtaining quasi-identical transport matrices through various elements or sections of the AtR was a preliminary check in constructing its model in Zgoubi. They are made available here, for possible further investigations, or to serve as guidance in reproducing the numerical simulations discussed in this report.

Details can be found in the corresponding Zgoubi I/O data files, archived at

$$/rap/lattice\_tools/zgoubi/AgsZgoubiModel/AtR/n0$$

UTV1

```
      1.00000        0.609600        2.559518E-22   -5.201971E-23     0.00000        1.526061E-17
   -1.715069E-10     1.00000         8.397986E-22    2.559530E-22     0.00000        5.006761E-17
   -6.588358E-18     3.859408E-17    1.00000         0.609600         0.00000        3.116579E-06
    8.397986E-22     1.086082E-16    0.00000         1.00000          0.00000        1.022500E-05
    0.00000          0.00000         1.022500E-05    3.116511E-06     1.00000        1.136868E-11

      1.000000        0.609600        0.000000        0.000000        0.000000        0.000000
      0.000000        1.000000        0.000000        0.000000        0.000000        0.000000
      0.000000        0.000000        1.000000        0.609600        0.000000        0.000003
      0.000000        0.000000        0.000000        1.000000        0.000000        0.000010
      0.000000        0.000000       -0.000010       -0.000003        1.000000        0.000000
```

At U end

```
 Reference, absolute (part #   1)  :   0.00000E+00 -3.39595E-05  9.91799E-06  6.69600E-14  4.26278E-14  1.60102E+04   5.34456E-01

          Frame for MATRIX calculation moved by :
           XC =    0.000 cm , YC =    0.000 cm ,   A =  0.00000 deg  ( = 0.000000 rad )


 Reference particle (#   1), path length :   16010.154     cm  relative momentum :    1.00000


                 TRANSFER  MATRIX  ORDRE  1  (MKSA units)

        -2.36013         20.7414       -7.079628E-05    6.222565E-04     0.00000       -0.811218
        0.117499        -1.45632        3.524872E-06   -4.368670E-05     0.00000       -1.483158E-02
        3.717167E-05   -2.867280E-04    -1.23961         9.56371         0.00000        1.406942E-04
        3.608548E-06   -3.636979E-06   -0.120321        0.121584         0.00000        5.501942E-06
        0.130322        -1.48902        1.401531E-05   -9.167707E-06     1.00000       -5.482084E-02
         0.00000         0.00000         0.00000         0.00000         0.00000         1.00000

  begin UEND       1    96.553340    96.553340      -7.552935     -0.001177     96.173097      -0.214890     -0.000016      0.000027

       -2.360140       20.742503       -0.000071        0.000622        0.000000       -0.810920
        0.117499       -1.456363        0.000004       -0.000044        0.000000       -0.014843
        0.000037       -0.000287       -1.239628        9.563646        0.000000        0.000141
        0.000004       -0.000004       -0.120324        0.121597        0.000000        0.000006
       -0.130313        1.488866       -0.000014        0.000009        1.000000        0.054865
        0.000000        0.000000        0.000000        0.000000        0.000000        1.000000
```

WD1

```
 Reference, absolute (part #   1)  :   0.00000E+00  6.42297E-07  3.60517E-06  0.00000E+00  0.00000E+00  3.65789E+02   1.22014E-02

          Frame for MATRIX calculation moved by :
           XC =    0.000 cm , YC =    0.000 cm ,   A =  0.00000 deg  ( = 0.000000 rad )


 Reference particle (#   1), path length :   365.78871     cm  relative momentum :    1.00000


                 TRANSFER  MATRIX  ORDRE  1  (MKSA units)

         1.16151         3.85156         0.00000         0.00000         0.00000        8.191088E-02
        9.063846E-02     1.16151         0.00000         0.00000         0.00000        4.596864E-02
         0.00000         0.00000        0.845842         3.46906         0.00000         0.00000
         0.00000         0.00000       -8.202543E-02    0.845842        0.00000         0.00000
        4.596864E-02    8.191088E-02     0.00000         0.00000         1.00000        1.185131E-03
         0.00000         0.00000         0.00000         0.00000         0.00000         1.00000

  139 W20DEGRE   1   160.102  begin RMATRIX range
  140 WDIP1      1   163.759  end   RMATRIX range
        1.161495        3.851560        0.000000        0.000000        0.000000        0.081900
        0.090631        1.161495        0.000000        0.000000        0.000000        0.045962
        0.000000        0.000000        0.845853        3.469059        0.000000        0.000000
        0.000000        0.000000       -0.082020        0.845853        0.000000        0.000000
       -0.045962       -0.081900        0.000000        0.000000        1.000000       -0.001178
        0.000000        0.000000        0.000000        0.000000        0.000000        1.000000
```

WP1

```
  Reference, absolute (part #   1)  :   0.00000E+00  1.48386E-26  1.52896E-25  3.03040E-15  3.12250E-14  1.82881E+02   6.1002
6E-03

          Frame for MATRIX calculation moved by :
           XC =    0.000 cm , YC =    0.000 cm ,   A =  0.00000 deg  ( = 0.000000 rad )


  Reference particle (#   1), path length :   182.88119     cm  relative momentum :    1.00000


                TRANSFER  MATRIX  ORDRE  1  (MKSA units)

         0.999922         1.82881        3.831161E-16   -2.335443E-16     0.00000        5.600897E-14
        -8.556196E-05     0.999922       4.189618E-16    3.831161E-16     0.00000        6.125335E-14
        -1.131999E-14     6.899973E-13    1.00000         1.82876         0.00000        1.143836E-02
        4.189618E-16    3.079647E-13   -1.893266E-27     1.00000         0.00000        1.250939E-02
          0.00000         0.00000        1.250939E-02    1.143837E-02     1.00000        4.769529E-05
          0.00000         0.00000         0.00000         0.00000         0.00000         1.00000


   144 WCOR1      1   187.580  begin RMATRIX range
   145 WP1        1   189.409  end   RMATRIX range
         0.999922        1.828812        0.000000        0.000000        0.000000        0.000000
        -0.000086        0.999922        0.000000        0.000000        0.000000        0.000000
         0.000000        0.000000        1.000000        1.828764        0.000000        0.011438
         0.000000        0.000000        0.000000        1.000000        0.000000        0.012509
         0.000000        0.000000       -0.012509       -0.011438        1.000000       -0.000047
         0.000000        0.000000        0.000000        0.000000        0.000000        1.000000
```

WROLL+WD3

```
 Reference, absolute (part #   1)  :   0.00000E+00  6.42297E-07  3.60517E-06  0.00000E+00  0.00000E+00  3.65789E+02   1.2201
4E-02

          Frame for MATRIX calculation moved by :
           XC =    0.000 cm , YC =    0.000 cm ,   A =  0.00000 deg  ( = 0.000000 rad )


  Reference particle (#   1), path length :   365.78871     cm  relative momentum :    1.00000


                TRANSFER  MATRIX  ORDRE  1  (MKSA units)

          1.16151         3.85156        3.137232E-04    1.040306E-03     0.00000        8.191088E-02
         9.063846E-02     1.16151        2.448145E-05    3.137232E-04     0.00000        4.596864E-02
        -2.284619E-04   -9.369944E-04    0.845842         3.46906         0.00000         0.00000
         2.215507E-05   -2.284619E-04   -8.202542E-02    0.845842        0.00000         0.00000
         4.596864E-02    8.191088E-02    1.241631E-05    2.212289E-05     1.00000        1.185131E-03
          0.00000         0.00000         0.00000         0.00000         0.00000         1.00000


   146 WDIP3      1   195.521  begin RMATRIX range
   148 WD3        1   199.179  end   RMATRIX range
         1.161495        3.851560        0.000314        0.001040        0.000000        0.081900
         0.090631        1.161495        0.000024        0.000314        0.000000        0.045962
        -0.000228       -0.000937        0.845853        3.469058        0.000000        0.000000
         0.000022       -0.000228       -0.082020        0.845853        0.000000        0.000000
        -0.045962       -0.081900       -0.000012       -0.000022        1.000000       -0.001178
         0.000000        0.000000        0.000000        0.000000        0.000000        1.000000
```

WROLL+WD8

```
 Reference, absolute (part #   1)  :   0.00000E+00  1.52109E-06  8.10073E-06  0.00000E+00  0.00000E+00  3.65789E+02   1.2201
4E-02

          Frame for MATRIX calculation moved by :
           XC =    0.000 cm , YC =    0.000 cm ,   A =  0.00000 deg  ( = 0.000000 rad )


  Reference particle (#   1), path length :   365.78932     cm  relative momentum :    1.00000


                TRANSFER  MATRIX  ORDRE  1  (MKSA units)

         0.846744         3.46793        2.287056E-04    9.366888E-04     0.00000        7.772633E-02
        -8.161184E-02     0.846744      -2.204336E-05    2.287056E-04     0.00000        4.139082E-02
        -3.134525E-04   -1.040628E-03     1.16051         3.85275         0.00000         0.00000
        -2.431076E-05   -3.134525E-04    9.000652E-02     1.16051         0.00000         0.00000
         4.139082E-02    7.772632E-02    1.117985E-05    2.099512E-05     1.00000        1.136443E-03
          0.00000         0.00000         0.00000         0.00000         0.00000         1.00000


   188 WDIP8      1   284.069  begin RMATRIX range
   190 WD8        1   287.727  end   RMATRIX range
         0.846756        3.467934        0.000229        0.000937        0.000000        0.077715
        -0.081606        0.846756       -0.000022        0.000229        0.000000        0.041385
        -0.000313       -0.001041        1.160492        3.852758        0.000000        0.000000
        -0.000024       -0.000313        0.089998        1.160492        0.000000        0.000000
        -0.041385       -0.077715       -0.000011       -0.000021        1.000000       -0.001141
         0.000000        0.000000        0.000000        0.000000        0.000000        1.000000
```

Start to WDRIFTN3

```
  Reference, absolute (part #   1)  :   0.00000E+00  6.67392E-05 -4.78610E-05 -5.25380E-08  2.61136E-07  3.89817E+04   1.30130E+00

          Frame for MATRIX calculation moved by :
           XC =    0.000 cm , YC =    0.000 cm ,   A =  0.00000 deg  ( = 0.000000 rad )


  Reference particle (#   1), path length :   38981.683     cm  relative momentum :    1.00000


                 TRANSFER  MATRIX  ORDRE  1  (MKSA units)

          3.21791        -15.8509        2.665085E-02    7.015612E-02     0.00000         2.72274
         -0.255431         1.56896       -1.528834E-03   -3.172576E-03     0.00000        -0.175683
         -5.028781E-04   -1.379963E-02     1.53674         6.01064         0.00000        -2.761281E-03
          1.221052E-03   -1.164333E-02    2.260348E-02     0.739124        0.00000         1.959647E-04
          0.130145        -1.48720        -1.559420E-04   -4.684262E-04    1.00000         0.483998
          0.00000          0.00000         0.00000         0.00000         0.00000         1.00000


     0 *LIN.03*   1     0.000  begin RMATRIX range
   239 WDRIFTN3   1   389.817  end   RMATRIX range
         3.221422      -15.886694        0.026646        0.070060        0.000000        2.724637
        -0.255618        1.571017       -0.001528       -0.003167        0.000000       -0.175762
        -0.000506       -0.013772        1.536916        6.007555        0.000000       -0.002719
         0.001221       -0.011642        0.022699        0.739365        0.000000        0.000196
        -0.130266        1.488205        0.000156        0.000499        1.000000       -0.483932
```

YD1

```
  Reference, absolute (part #   1)  :   0.00000E+00 -1.01109E-06 -5.76150E-06  0.00000E+00  0.00000E+00  3.65795E+02   1.2201
6E-02

          Frame for MATRIX calculation moved by :
           XC =    0.000 cm , YC =    0.000 cm ,   A =  0.00000 deg  ( = 0.000000 rad )


  Reference particle (#   1), path length :   365.79475     cm  relative momentum :    1.00000


                 TRANSFER  MATRIX  ORDRE  1  (MKSA units)

          1.26586         3.97519         0.00000         0.00000         0.00000         9.188868E-02
         0.151539         1.26586         0.00000         0.00000         0.00000         5.237653E-02
          0.00000         0.00000         0.754730        3.35508         0.00000         0.00000
          0.00000         0.00000        -0.128278        0.754730        0.00000         0.00000
         5.237653E-02    9.188868E-02     0.00000         0.00000         1.00000         1.462553E-03
          0.00000         0.00000         0.00000         0.00000         0.00000         1.00000


   247 YDIP1      1   403.412  begin RMATRIX range
   248 YD1        1   407.070  end   RMATRIX range
         1.265833        3.975193        0.000000        0.000000        0.000000        0.091857
         0.151523        1.265833        0.000000        0.000000        0.000000        0.052358
         0.000000        0.000000        0.754752        3.355064        0.000000        0.000000
         0.000000        0.000000       -0.128269        0.754752        0.000000        0.000000
        -0.052358       -0.091857        0.000000        0.000000        1.000000       -0.001449
         0.000000        0.000000        0.000000        0.000000        0.000000        1.000000
```

U+W+Y

```
  Reference, absolute (part #   1)  :   0.00000E+00  1.70130E-05 -7.13780E-07  1.89196E-07  8.03969E-08  5.81026E+04   1.93960E+00

          Frame for MATRIX calculation moved by :
           XC =    0.000 cm , YC =    0.000 cm ,   A =  0.00000 deg  ( = 0.000000 rad )


  Reference particle (#   1), path length :   58102.556     cm  relative momentum :    1.00000


                 TRANSFER  MATRIX  ORDRE  1  (MKSA units)

         -2.78658         17.2839        -1.634554E-02   -3.317544E-02     0.00000        -2.72892
        -3.943743E-02    -0.114243       -9.113736E-04   -3.247090E-03     0.00000        -0.122805
         1.015341E-02    -0.108648         1.18162         10.1841         0.00000         2.038338E-02
         1.604150E-04     5.329748E-04    -0.167967       -0.601396        0.00000         3.590480E-03
         0.234618         -2.43472         7.186456E-03    4.403697E-02    1.00000         2.88865
          0.00000          0.00000         0.00000         0.00000         0.00000         1.00000

        DetY-1 =      -0.0000228647,    DetZ-1 =      -0.0000228655


    0 *LIN.03*   1     0.000  begin RMATRIX range
   402 *LIN.03*   1   581.026  end   RMATRIX range
        -2.796068       17.367809       -0.016356       -0.033083        0.000000       -2.731881
        -0.039314       -0.113439       -0.000908       -0.003232        0.000000       -0.122564
         0.010130       -0.108475        1.184844       10.183857        0.000000        0.020402
         0.000161        0.000527       -0.168178       -0.601530        0.000000        0.003586
        -0.235330        2.438970       -0.007205       -0.044019        1.000000       -2.887779
```

B Zgoubi data for $\vec{n}_0$ search

Excerpt of zgoubi.dat input data file, including "FIT" and its appropriate arguments, as used for finding the stable spin vector $\vec{n}_0$ in the AGS. The snakes are shown explicitly for clarity (maps used, settings, etc.).

A complete zgoubi.dat template is available in the AGS Zgoubi model development area, namely

/rap/lattice_tools/zgoubi/AgsZgoubiModel/templateZgoubi4ZgoubiFromSnaprampCmd_library/ppmUser4_pp/templateZgoubi4ZgoubiFromSnaprampCmd.dat

```
Template zgoubi.dat. 2 snakes.
 'OBJET'     LBL_OBJfit
79.2855199D3
2
1 1
0. 0. 0. 0. 0. 1. 'o'
1
 'PARTICUL'
938.27203   1.602176487E-19  1.7928474 0. 0.
 'SPNTRK'
4.1
0. 0. 1.
 'SCALING'   POWER SUPPLIES
1   14
AGSMM *AF *BF *CF !dB0 (FIT#3), dB1(FIT# 4), dB2   MAIN MAGNETS
-1          3      13    3.E-20 14   4e-20   15   5.E-20
1.000000006    ! (FIT #6)
1
AGSMM *AD *BD *CD !dB0 (FIT#9), dB1(FIT#10), dB2   MAIN MAGNETS
-1          3      13    9.E-20 14   10e-20  15  11.E-20
1.00000012    ! (FIT#12)
1
AGSQUAD  QH_*                                      H TUNE QUADS
-1
1.00000015    ! (FIT#15)
1
AGSQUAD  QV_*                                      V TUNE QUADS
-1
1.00000018    ! (FIT#18)
1
MULTIPOL COH1                                   COLD SNAKE BUMP
1.10
./Csnk3D/Hlx68.2_Sol42.3/bump_centered.scal
1 2
MULTIPOL COV1
1.10
./Csnk3D/Hlx68.2_Sol42.3/bump_centered.scal
1 3
MULTIPOL COH2
1.10
./Csnk3D/Hlx68.2_Sol42.3/bump_centered.scal
1 4
MULTIPOL COV2
1.10
./Csnk3D/Hlx68.2_Sol42.3/bump_centered.scal
1 5
MULTIPOL WOH1                                   WARM SNAKE BUMP
1.10
./Wsnk3D/bump_centered.scal
1 2
MULTIPOL WOV1
1.10
./Wsnk3D/bump_centered.scal
1 3
MULTIPOL WOH2
1.10
./Wsnk3D/bump_centered.scal
1 4
MULTIPOL WOV2
1.10
./Wsnk3D/bump_centered.scal
1 5
MULTIPOL HKICE VKICE
1
1.00000015
1
MULTIPOL   OTHER LENSES
-1
79.2855199
1
```

```
 'MARKER'   #Start                       START OF AGS SEQUENCE
 'AGSMM'  MM_A01BF
0
3 0 0   1.00000E+00  1.00000E+00  1.00000E+00
2  1 0.  1 0.
0. 0. 10.00  4.0  0.800 0.00 0.00 0.00 0.00 0. 0. 0. 0.
4  .1455   2.2670  -.6395  1.1558  0. 0.  0.
0. 0. 10.00  4.0  0.800 0.00 0.00 0.00 0.00 0. 0. 0. 0.
4  .1455   2.2670  -.6395  1.1558  0. 0.  0.
0. 0. 0. 0. 0. 0. 0. 0. 0. 0.
10.0  Dip MM_A01BF
3  0. -0.3942767  0.011751150  angle =  -0.02350230 rad
.................................
... DOWN TO THE COLD SNAKE    ....
.................................
 'DRIFT'         94
-20.
 'TOSCA'         95
0  2                        ** New field maps, length=+/-1.6m.
10.15 1. 1. 1.              ** 10.15 yields same precession as full hlx+sol map.
HEADER_9                    ** 68% hlx : 0.9578 = 68/71.
321 29 29 15.2 0.9578 0.216 ** 76A sol/68.2%hlx -> 76/350*(68/68.2)^2=0.216/68%hlx.
Csnk3D_map/b_ags-full-coilv5-x06-rerun2-x071-integral-x5y5z10mm.table
Csnk3D_map/b_ags-full-sold3-only-nodal-x5y5z10mm-wasActually-integral.table
0 0 0 0
2
.1
2  0.  .00  0.  0.
 'DRIFT'         96
-20.
.................................
... DOWN TO THE WARM SNAKE    ....
.................................
 'TOSCA'        418
0  0
1.e1   100. 100. 100.
HEADER_0 wsnake
801 29 29 15.1 1.
Wsnk3D_map/b_table55.TAB
0 0 0 0
2
.1
2  0.  .00  0.  0.
.................................
... THE REST OF THE AGS RING  ....
.................................

 'AGSMM'  MM_L20BD
0
3 0 0   1.00000E+00  1.00000E+00  1.00000E+00
2  1 0.  1 0.
0. 0. 10.00  4.0  0.800 0.00 0.00 0.00 0.00 0. 0. 0. 0.
4  .1455   2.2670  -.6395  1.1558  0. 0.  0.
0. 0. 10.00  4.0  0.800 0.00 0.00 0.00 0.00 0. 0. 0. 0.
4  .1455   2.2670  -.6395  1.1558  0. 0.  0.
0. 0. 0. 0. 0. 0. 0. 0. 0. 0.
10.0  Dip MM_L20BD
3  0.  -0.3917463  0.011751150  angle =  -0.02350230 rad
 'DRIFT' DRIF D10                DRIF
152.3839
 'DRIFT' DRIF D10                DRIF
152.3839
 'MARKER'   #End          958
 'FAISCEAU'                                  END OF AGS SEQUENCE

 'FIT'                    960
3                          ! Variables
3  10  0  [-1., +1.]       !   Vary n_X at start
3  11  0  [-1., +1.]       !   Vary n_Y     "
3  12  0  [-1., +1.]       !   Vary n_Z     "
4    1.0000E-08   1000     ! Constraints
10.1 1 1 961 0. 1.  0      !   n_X(initial) = n_X(final)
10.1 1 2 961 0. 1.  0      !   n_Y(initial) = n_Y(final)
10.1 1 3 961 0. 1.  0      !   n_Z(initial) = n_Z(final)
10   1 4 961 1. .01 0      !   |n|=1

     'END'
```

References

[1] Where are the AGS snakes ? F. Méot et al., Tech. Note C-A/AP/485, July 2013.

[2] Spin transport from AGS to RHIC with two partial snakes in AGS, W. MacKay et al., Procs. EPAC 2006 Acc. Conf., Edinburgh.

[3] Closed orbit calculations at AGS and extraction beam parameters at H13, N. Tsoupas et al., Tech Note AD/RHIC/RD-75, Oct. 1994.

[4] Stable spin direction of a polarized proton beam at the injection point of RHIC, N. Tsoupas et al., Spin Note AGS/RHIC/SN 021, March 1996.

[5] The ray-tracing code Zgoubi, http://sourceforge.net/projects/zgoubi/
Zgoubi Users' Guide, F. Méot, Report CA/AP/470, BNL C-AD, Oct. 2012.

[6] Development of a stepwise ray-tracing based on-line model at AGS, F. Méot et al., Procs. PAC 2011 Acc. Conf., NY.
Modelling of the AGS using Zgoubi - status, F. Méot et al., Procs. IPAC 2011 Acc. Conf., San Sebastian.

[7] Helical dipole partial snakes for the AGS, J. Takano et al., JINST1, P11002 (2006).